Improving the tolerance to alkali and alkaline earth metal chlorides of WO3 and Nb2O5 promoted V2O5/TiO2 catalysts for the NH3-SCR reaction

Improving the tolerance to alkali and alkaline metal chlorides of WO_3 and Nb_2O_5 promoted V_2O_5/TiO_2 catalysts for the NH_3-SCR reaction

Jun Cao [a,b], *Chiara Nannuzzi* [b], *Weizao Liu* [a,*], *Hongli Wu* [a], *Yuxiang Gao* [a], *Rigang Zhong* [a,c], *Qingcai Liu* [a,*], *Gloria Berlier* [b,*]

[a] College of Materials Science and Engineering, Chongqing University, Chongqing 400044, PR China

[b] Department of Chemistry and NIS Centre, University of Turin, via P. Giuria 7, 10125, Turin, Italy

[c] Shenzhen Energy Environment, Co., LTD, Shenzhen 518055, PR China.

*Corresponding author at: College of Materials Science and Engineering, Chongqing University, Shazheng street 174#, Chongqing 400044, PR China.

Tel.: +86 23 65127302.

E-mail address: liuwz@cqu.edu.cn (W.Z. Liu), liu_qingcai@163.com (Q.C. Liu).

*Corresponding author at: Department of Chemistry and NIS Centre, University of Turin, via P. Giuria 7, 10125, Turin, Italy.

Tel.: +39 0116707856

E-mail address: gloria.berlier@unito.it

Abstract

V_2O_5-WO_3/TiO_2 catalysts are widely used to reduce NO_x emissions from municipal solid

waste incineration. However, the flue gas always contains different alkali (and alkaline earth) metal chlorides. In this work, we compared the effect of KCl, NaCl and $CaCl_2$ on V_2O_5-WO_3/TiO_2 catalyst for the NH_3 Selective Catalytic Reduction of NO_x, and we aim to improve the tolerance of the catalyst by replacing WO_3 with Nb_2O_5. It was found that KCl has the greatest poisoning effect, resulting in a severe decrease in the surface acidity, redox performance, V^{5+}/V^{4+} ratio and surface adsorbed oxygen. The replacement of WO_3 with Nb_2O_5 improved the activity and KCl tolerance of the catalyst owing to the improvement of surface acidity, redox performance, and V^{5+} ratio and surface adsorbed oxygen. This may be due to that Nb_2O_5 is easier to bond with K than that of V_2O_5, protecting V_2O_5 more effectively. *In-situ* DRITFS experiments showed that alkali (earth) metal ions favor the transformation of adsorbed NO_2 species into stable nitrates and nitrites. However, the replacement of WO_3 with Nb_2O_5 would inhibit the formation of these stable species owing to the larger surface adsorbed oxygen.

Keywords: V_2O_5 -WO_3/TiO_2; Alkali metal chlorides poisoning; Replacement of Nb_2O_5; KCl tolerance; NH_3-SCR

1 Introduction

With the rapid economic development and improvement of living standards, a large amount of domestic waste is discharged in the environment [1]. Notwithstanding the general increase in recycling and composting procedures (and corresponding processed waste volume), the waste incineration technology is still regarded as an effective way to quickly eliminate waste. The ammonia-Selective Catalytic Reduction (NH_3-SCR) technology is widely used to control the emission of NO_x from municipal solid waste incineration flue gas, and NH_3-SCR catalysts are the key unit for this technology [2, 3]. A large number low-temperature NH_3-SCR catalyst have been studied, such as CeO_2-MnO_2, MnO_2-TiO_2, CeO_2-TiO_2, and MnO_2-FeO_2, etc [4-9]. However, V_2O_5-WO_3/TiO_2 (where V_2O_5 is the active phase and WO_3 is a promoter) is still the commercial deNO_x catalyst owing to its efficient activity and excellent resistance to H_2O and SO_2 [10-12].

Compared with the catalyst used in coal-fired power plants, the V_2O_5 content of the catalyst used in waste incineration plants is larger, usually 3wt% vs 1wt% in the coal-fired power plants. This is mainly due to the difference in the temperature of the NH_3-SCR process, which is usually around 400 ^oC and 215 ^oC in coal-fired power plant and waste incineration one, respectively. Moreover, the flue gas from waste incineration plants always contains K, Na, Ca, Cl, Pb, Zn, etc, which would lead to the serious deactivation of the catalyst [4].

The effect of alkali (and alkaline earth) metal oxides on the activity of V_2O_5-WO_3/TiO_2 catalyst has been studied extensively [13-15]. Chen et al [16] compared the effect of Na_2O, K_2O, MgO, and CaO on V_2O_5-WO_3/TiO_2 catalyst, and it was found that the degree of poisoning effect was related to the alkalinity of the metals, *i.e.*, K_2O>Na_2O>CaO>MgO. This was explained in terms of greater decrease in the amount of Brønsted acid sites and reducibility of V_2O_5 and WO_3 species for K_2O with respect to the other oxides. Du et al. [17] studied the poisoning effect of alkali oxide by density functional theory (DFT) calculations on VO_4H_3 clusters. The authors computed a competition between alkali hydroxides neutralization and NH_3 adsorption with surface V-OH

Brønsted acid sites, resulting in a decrease of acidity and corresponding NH_3 sorption capacity. Moreover, the replacement of hydrogen with alkali metal ions in the VO_4H_3 cluster after neutralization led to the reduction of V^{5+} species, resulting in a decrease the redox performance of the catalyst. Similar conclusions were drawn by Peng et al. [18], who studied by DFT V_2O_5/TiO_2 and WO_3/TiO_2 (001) surface models. The presence of K ions would lower NH_3 adsorption by occupying the Brønsted acid sites and weakening the Lewis ones. Moreover, surface K ions would lower the reducibility of the V_2O_5 active phase, rather than the promoter WO_3.

As we known, a large amount of Cl ions is present in the flue gas from waste incineration plants, which would form alkali (and alkaline earth) metal chlorides. Some researchers found that alkali metal chlorides had a greater poisoning effect on V_2O_5-WO_3/TiO_2 catalyst than alkali metals oxides [19]. Therefore, it is of great significance to compare the effect of different alkali metal chlorides on V_2O_5-WO_3/TiO_2 catalysts with high vanadium content and to improve their resistance to alkali metal chlorides.

Nb_2O_5 is also widely used as a promoter in the catalysts for alkane hydrogenation and NH_3-SCR reactions [20, 21]. It was found that the addition of Nb_2O_5 would improve the surface acidity and redox performance of the catalyst [22, 23]. Moreover, Kröcher et al. [24] found that the addition of Nb_2O_5 dramatically enhanced the activity and N_2 selectivity of MnO_2-CeO_2 catalyst in NH_3-SCR owing to the strong interaction between Nb and Mn, which led to a remarkable dispersion of the redox and acidic sites. Nb_2O_5 was also found to improve the amount of surface adsorbed oxygen in the CeO_2-Nb_2O_5 catalyst, which has been related to a short-range activation effect of Nb_2O_5 to CeO_2 species [21, 25-27]. However, to our knowledge the effect of Nb_2O_5 promoter on alkali chloride tolerance of V_2O_5/TiO_2 catalysts for NH_3-SCR performance has not been studied up to now.

In this work, the effect of different alkali (and alkaline earth) metal chlorides (NaCl, KCl and $CaCl_2$) on the NH_3-SCR performance and physicochemical properties of a V_2O_5-WO_3/TiO_2 catalyst

was compared. The substitution of the WO_3 promoter with Nb_2O_5 was investigated in relation to KCl tolerance of the catalyst. The catalysts were characterized about their general physicochemical properties (crystal phase, surface area and porosity), surface composition and acidity, reducibility of the V_2O_5 active phase and WO_3/Nb_2O_5 promoters. The results are discussed in relation to the decrease of catalytic activity induced by the different alkali (and alkaline earth) metal chlorides.

2. Experimental

2.1 Preparation of catalysts

V_2O_5-WO_3/TiO_2 catalyst was prepared by impregnation method with the mass ratio of V_2O_5 and WO_3 of 3.0% and 5.0%, respectively. This corresponds to 2.5 V_{at}/nm^2 and 1.6 W_{at}/nm^2 (see Table 1 for textural properties). In detail, the required amount of NH_4VO_3, $H_{40}N_{10}O_{41}W_{12}$ ·xH_2O and $C_2H_2O_4{\cdot}2H_2O$ were added into 20 mL ultrapure water and mixed well to form the solution, in which the molar ratio of NH_4VO_3/ $C_2H_2O_4{\cdot}H_2O$ was 1:2. Then TiO_2 was added into the mixed solution, and the solvent was evaporated in a water bath at 90 ^oC with stirring. Finally, the sample was calcined at 450 ^oC for 5 h, and labeled as VWTi.

The poisoned VWTi catalysts were made by impregnation method using a KCl, NaCl or $CaCl_2$ solution (2.0wt%, corresponding to 2.7×10^{-4}, 3.4×10^{-4}, 1.8×10^{-4} mol/g, respectively), which was evaporated at 90 ^oC in a water bath with continuous stirring. The obtained samples were labeled as KCl-VWTi, NaCl-VWTi and $CaCl_2$-VWTi, respectively.

For comparison, V_2O_5-Nb_2O_5/TiO_2 (labeled as VNbTi) and KCl-poisoned V_2O_5-Nb_2O_5/TiO_2 (labeled as KCl-VNbTi) were also prepared by the same method, where $H_{40}N_{10}O_{41}W_{12}$ was replaced by $C_{10}H_5NbO_{20}{\cdot}xH_2O$ (5 wt% Nb_2O_5 in the catalyst).

2.2 NH_3-SCR performance evaluation

The NH_3-SCR performance of these catalysts was measured in a fixed-bed reactor (quartz tube

with the length of 500 mm and inner diameter of 8 mm) using 0.2 g catalyst with particle size of 20-60 mesh. The feed gas contained 1000 ppm NO, 1000 ppm NH_3, and 11 vol.% O_2 and N_2 as the balanced gas, with a total flow rate of 300 mL/min. The catalyst was purged with N_2 at 300 °C for 0.5 h before the test. The outlet gas concentration (NO_x, NH_3, N_2O) was analyzed by an Gasmet FTIR DX-4000 infrared gas detector. The NO_x conversion and N_2 selectivity were calculated by following eqs:

$$NO_x \text{ conversion } (\%)=\left(1-\frac{[NO_x]_{out}}{[NO_x]_{in}}\right)\times 100\% \quad (1)$$

$$N_2 \text{ Selectivity } (\%)=\left(1-\frac{2[N_2O]_{out}}{[NO_x]_{in}+[NH_3]_{in}-[NO_x]_{out}-[NH_3]_{out}}\right)\times 100\% \quad (2)$$

2.3 Catalyst characterization

A PANnalytical X' Pwet Powder diffractometer was chosen to measure the XRD patterns of the fresh and poisoned catalysts, operating at 40 KV and 40 mA using a Ni-filtered Cu Kα radiation.

Raman spectra were collected with a Renishaw micro-Raman spectrometer, equipped with a 785 nm diode laser (Renishaw) as the excitation source. The laser was focused on the sample through a 20×long working distance objective, which also captures the backscattered light. The elastically scattered light was filtered by an edge filter, and the Stoke-scattered portion was dispersed by a 1200 lines/mm grating and passed to a Peltier-cooled CCD for detection. Before the measurements, the catalysts were placed in a capillary and dehydrated by a thermal tratement at 450°C for 2h in a static oven. The capillary were sealed before the measurements to avoid exposure to ambient conditions. The spectra were normalized to the intensity of the TiO_2 support band at 144 cm^{-1}.

The texture of the samples was analyzed by N_2-physisorption at the liquid nitrogen temperature (-196 °C) using a Micromeritics ASAP 2010 instrument. The specific surface area of samples was calculated by the Brunauer-Emmett-Teller (BET) method; total pore volume and mean pore diameter were calculated by the Barrett-Joyner-Halenda (BJH) method.

NH_3-TPD experiments were performed on the activity evaluation device, and the concentration of NH_3 was analyzed by the Gasmet FTIR DX-4000 infrared gas detector. First, 0.1 g sample was purged at 300 ^oC with N_2 for 30 min, cooled to room temperature (30 ^oC), and then contacted with NH_3. After saturation, the samples were purged with N_2 until the concentration of NH_3 dropped to 0 ppm. Finally, the desorption process was started from 30 ^oC to 550 ^oC under N_2 with a ramp rate of 10 ^oC/min.

A chemisorption analyzer (TP-5076) was used to characterize the redox performance of these samples. First, 0.05 g sample was pretreated by He gas flow at 300 ^oC 1 h. After cooling to room temperature, the reduction process was started under 5% H_2/He with a rate of 10 °C/min.

XPS experiments were performed on a Thermo Scientific ESCALAB 250Xi with Al Kα X-ray radiation (1486.6 eV) at 150 W, and the Binding Energy was calibrated to the C 1s peak at 284.6 eV.

In-situ DRIFTs experiments were carried out with a Nicolet iS50 FT-IR spectrometer. Before the test, the sample was purged with N_2 at 300 ^oC for 30 min, and the sample was collected during the cooling process. Then, NH_3/N_2 ($NO+O_2/N_2$ or $NO+O_2+NH_3/N_2$) mixture was introduced until the sample was saturated. After that, the spectra were collected at each target temperature. The reported difference spectra were obtained by subtracting for each temperature the corresponding spectrum measured before dosing the mixture.

In-situ FTIR experiments in transmission mode were carried out to study the interaction of the CO probe molecule with the catalysts surface. The infrared spectra were measured with 4 cm^{-1} resolution on a Bruker Equinox 55 FTIR spectrometer, equipped with a mercury cadmium telluride (MCT) cryodetertor, Thin self-supporting wafers of each sample were placed inside an in-situ IR cell, which allowed for control of temperature and gas atmosphere. Before the measurements, the catalysts were treated at 500 ^oC for 2 h under dynamic vacuum, before admitting 80 mbar of O_2 at the same temperature. CO adsorption experiments were carried after cooling the cell with liquid nitrogen (estimated temperature under the IR beam -163 ^oC). The reported spectra of the catalysts

before CO dosage. All the spectra were normalized by using the optical density prepared pellets (weight of pellet divided by area).

3. Results and discussion

3.1 NH_3-SCR performance

The effect of different alkali and alkaline earth metal chlorides (KCl, NaCl, and $CaCl_2$) on the NH_3-SCR performance of VWTi catalysts in the 100-300 ^oC range was investigated, and the results are shown in Fig. 1. For VWTi catalyst, the NO_x conversion exceeded 85% above 225 ^oC, reaching about 99% at 300 ^oC. The NO_x conversion decreased after introducing KCl, NaCl, and $CaCl_2$, in the order of $CaCl_2$-VWTi > NaCl-VWTi > KCl-VWTi (84%, 64%, and 48% at 300 ^oC, respectively). 100% N_2 selectivity was achieved for all the fresh and poisoned catalysts (Fig.S1), which suggested that alkali and alkaline earth metal chlorides had no negative effect on N_2 selectivity of VWTi catalyst.

According to the above experimental results, it was found that KCl had the strongest poisoning effect on VWTi catalyst. On this basis, WO_3 was replaced by Nb_2O_5 to improve KCl tolerance of the vanadium-based catalyst. It was found that VNbTi catalyst had a better catalytic activity than VWTi, reaching nearly 96% at 225 ^oC, which was about 10% higher than that of VWTi catalyst. Moreover, VNbTi catalyst showed an excellent anti-KCl poisoning ability. After KCl poisoning, the NO_x conversion of VNbTi catalyst still reached about 80% at 300 ^oC, which was 1.7 times than that of VWTi catalyst. Also in this case no N_2O formation was observed during the reaction on VNbTi and KCl-VNbTi catalysts (as shown in Fig. S1). In summary, the replacement of WO_3 by Nb_2O_5 can effectively enhance the NH_3-SCR performance and KCl tolerance of the catalyst.

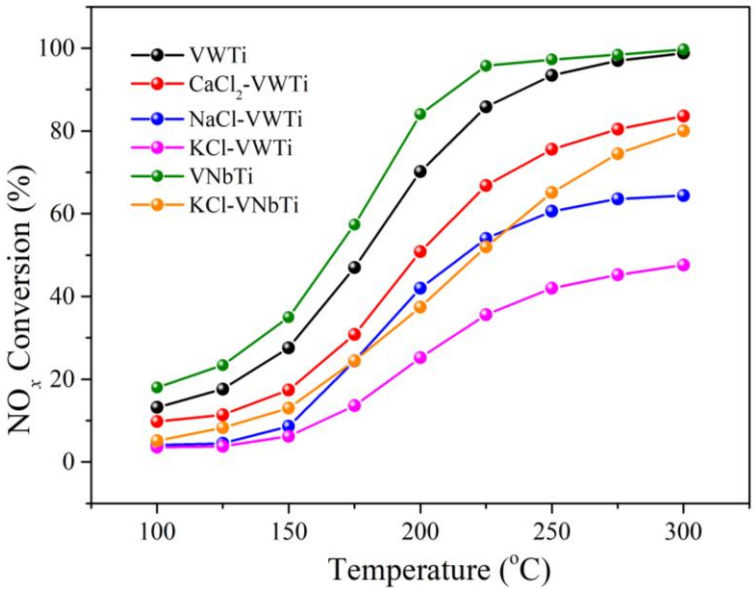

Fig. 1 The NH_3-SCR performance of the VWTi, VNbTi and corresponding alkali and alkaline earth metal chloride poisoned catalysts

3.2 General physico-chemical properties (XRD, Raman, and N_2-physisorption)

The crystal structure of the catalysts was analyzed by XRD, and the results are shown in Fig.S2. All samples showed the diffraction patterns of anatase TiO_2 phase without extra phases [PDF-ICDD-21-1272][28, 29]. This suggests the high dispersion of the active phase and the alkali/alkaline earth metal salts used for the poisoning.

The anatase phase of the samples was confirmed by Raman spectroscopy (Fig.2), showing for both fresh and poisoned catalysts bands at 143, 395, 515, and 619 cm^{-1} , which were assigned to the $E_{g(1)}$, $B_{1g(1)}$, $A_{1g}+B_{1g(2)}$, and $E_{g(2)}$ vibration modes of anatase TiO_2, respectively [30]. Moreover, three very weak bands appeared in the range of 950-1050 cm^{-1} over VWTi catalyst. The band at 1032 cm^{-1} can be related to the V=O stretching mode of the vanadyl species in the monomeric $O=V^{5+}O_3$ groups [31, 32], and the ones at 1015 and 1009 cm^{-1} to W=O stretching modes of di/oligomeric and isolated tungstenyl species, respectively [33, 34]. There is no evidence for the presence of crystalline V_2O_5 or WO_3 phases (sharp peaks expected at 998 and 800 cm^{-1}, respectively), indicating the good dispersion of the active phase.

After $CaCl_2$ poisoning, the vanadyl and tungstenyl bands are hardly affected, and new weak bands appear at 984 and 970 cm^{-1}. The interval 900-800 cm^{-1} is usually related to V-O-V vibrations, which are however observed at lower frequency (950-920 cm^{-1}) in dehydrated V_2O_5-TiO_2 samples [35]. The position of the bands, similar to what observed in hydrated VWTi samples [36] could suggest that V-O-V and V-O-W groups are perturbed by the presence of $CaCl_2$ on the surface.

On the other hand, Raman spectroscopy clearly shows a stronger perturbation of the VOx active phase and promoter by NaCl and KCl poisoning, since the bands at 1015 and 1032 cm^{-1} disappear, and a broad band grows at 984 cm^{-1}. These results indicate that KCl and NaCl have a stronger influence on the structure of VO_x surface species than $CaCl_2$. Also in this case no evidence for the peaks related to crystalline V_2O_5 or WO_3 were present in the spectra, indicating that the chloride salts did not promote sintering.

When Nb_2O_5 replaced WO_3 a band related to V=O stretching mode appeared at 1040 cm^{-1} owing to the presence of neighbor vanadyl species. This result indicates that replacing WO_3 with Nb_2O_5 can promote the interaction of VO_x species, resulting in the improvement of electron transfer ability, thereby enhancing the activity. Also in this case the presence of KCl suppresses the vanadyl bands, indicating a strong interaction of the cation with vanadyl groups.

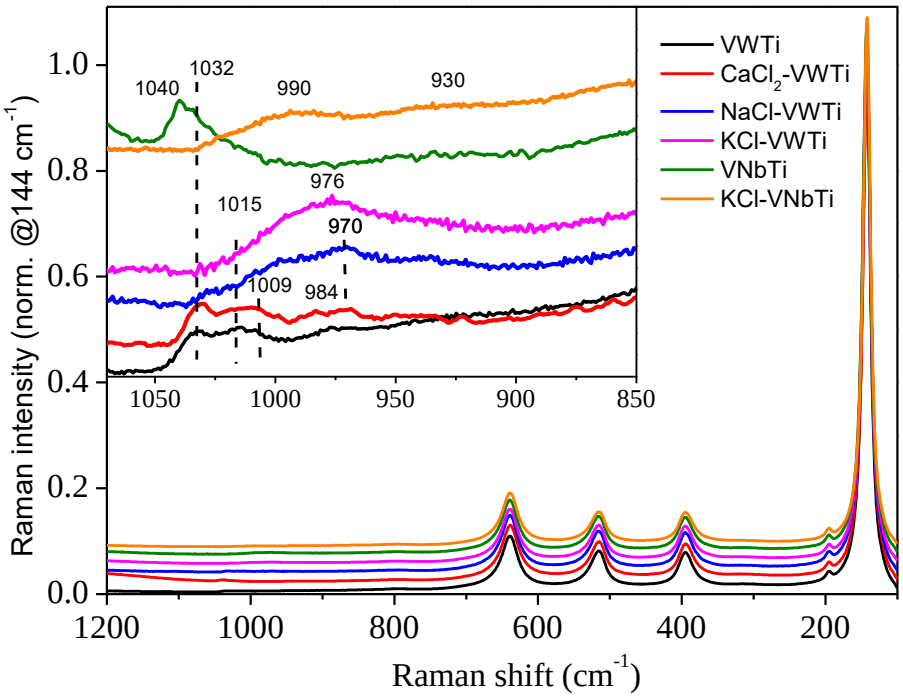

Fig. 2 Raman spectra of dehydrated VWTi, VNbTi and corresponding alkali and alkaline earth metal chloride poisoned catalysts.

The textural properties of the fresh and poisoned catalysts were measured by N_2-physisorption, and the results are displayed in Table 1. The BET specific surface area, total pore volume and mean pore diameter of VWTi catalyst were 79 m^2/g, 0.36 cm^3/g, and 9.1 nm, respectively. In general, a large surface area can promote the dispersion of active species, thereby improving the activity of the catalyst. The BET specific surface area of the catalysts is not particularly affected by the presence of the alkali and alkaline earth metal ions. The observed changes are within the experimental error. This suggests that the textural properties are not a key factor for the catalytic activity in this study.

Based on the measured values of surface area, the surface density of the active phase (V), promoters (W and Nb) and pollutants, expressed in at/nm^2 was calculated and reported in Table 2. The surface density of V is 2.5 at/nm^2 in all samples, with values around 4 and 5 at/nm^2 for V+W and V+Nb catalysts, respectively. These values do not exceed the theoretical monolayer, estimated

to be between 6 and 8 at/nm^2 for vanadium and 4.5 at/nm^2 for tungsten [31, 37]. This would imply a good dispersion of the active phase on the TiO_2 support surface, in agreement with XRD and Raman results. The surface density values reported in Table 2 show some variability, since they have been calculated with respect to the measured BET specific surface area of each sample (Table 1). However, we can safely state that all samples are characterized by the same VOx surface density.

The surface density of the chloride pollutants is between 1.3 and 2.6 at/nm^2 in the order $CaCl_2$<KCl<NaCl. This low amount points to an atomic dispersion of the metal ions and chlorine anions, excluding an aggregation effect on the active phase. No clear correlation is observed between the surface density of the metal ions (and chloride anions) and the SCR performance of the catalysts. More in detail, $CaCl_2$-VWTi has the lowest cation surface density and highest activity (1.3 at/nm^2 and 84% of NO_X conversion with respect to VWTi at 300 °C, respectively). However, the activity of KCl-VWTi (2.0 at/nm^2) is sensibly lower (48% of NO_X conversion) with respect to NaCl-VWTi with a slightly higher cations surface density (2.6 at/nm^2, 64% of NOx conversion).

Table 1 Textural properties of the VWTi, VNbTi and corresponding alkali and alkaline earth metal chloride poisoned catalysts.

Sample	BET specific surface area (m^2/g)	Total pore volume (cm^3/g)	Mean pore diameter (nm)
VWTi	79	0.36	9.1
$CaCl_2$-VWTi	83	0.37	11.8
NaCl-VWTi	81	0.36	11.7
KCl-VWTi	81	0.35	11.8
VNbTi	84	0.35	11.7
KCl-VNbTi	73	0.34	9.1

Table 2 Surface density of active phase and pollutants of the studied catalysts.

Sample	V (at/nm^2)	W/Nb (at/nm^2)	V+W/Nb (at/nm^2)	$MeCl_x$ (at/nm^2)	Total (at/nm^2)
VWTi	2.5	1.6	4.1	-	4.1
$CaCl_2$-VWTi	2.4	1.5	3.9	1.3	5.4
NaCl-VWTi	2.5	1.6	4.1	2.6	6.7
KCl-VWTi	2.5	1.6	4.1	2.0	6.2
VNbTi	2.4	2.7	5.1	-	5.1
KCl-VNbTi	2.7	3.1	5.8	2.2	8.0

3.3 Surface acidity (NH_3-TPD)

Surface acidity is regarded as an important factor to affect the activity of the catalysts in the NH_3-SCR reaction [38]. Therefore, NH_3-TPD was chosen to measure the surface acidity of these catalysts. Fig.3 shows the NH_3-TPD curves of the VWTi, VNbTi and corresponding poisoned catalysts. For VWTi, the TPD profile can be deconvoluted into three desorption peaks (*i.e.*, I, II, and III), which were related to the desorption of NH_3 from weak, medium and medium-strong acid sites, respectively [39, 40]. After poisoning, the amount of desorbed NH_3 decreases in the order VWTi>$CaCl_2$-VWTi>NaCl-VWTi>KCl-VWTi, as detailed in Table 3. The decrease is not correlated to the surface density of the salts (see Table 2), and indicates a chemical specificity of the pollutants in decreasing surface acidity of the catalysts, in agreement with the literature [16, 18, 41] . Indeed, we can observe that the decrease in the total amount of desorbed NH_3 from $CaCl_2$-VWTi is small (221 μmol/g vs 246 μmol/g in VWTi), but with a significant increase in the desorption temperature of medium-strong sites (403 vs 369 ^oC). On the other hand, the desorption peak related to medium-strong sites is shifted to lower temperature for NaCl-VWTi (329 ^oC) and absent in KCl-VWTi. The observed trend correlates well with the results of activity test, particularly concerning the total amount of acid surface sites probed by NH_3.

VNbTi catalyst shows an NH_3-TPD profile similar to that of VWTi, with similar desorption

temperature of the three deconvoluted components, and a higher total amount (284 μmol/g). Interestingly, also in this case KCl poisoning mainly affects the high temperature peak, which however does not disappear completely. In this case the total surface acidity of the poisoned KCl-VNbTi catalyst was about 60% of the starting material, which is larger than what measured for KCl-VWTi (46%). These results suggest that the replacement of WO_3 by Nb_2O_5 can improve the surface acidity of VWTi catalyst, and it effectively reduces the effect of KCl on the surface acidity of the catalyst, thereby enhancing the NH_3-SCR performance and resistance of KCl poisoning.

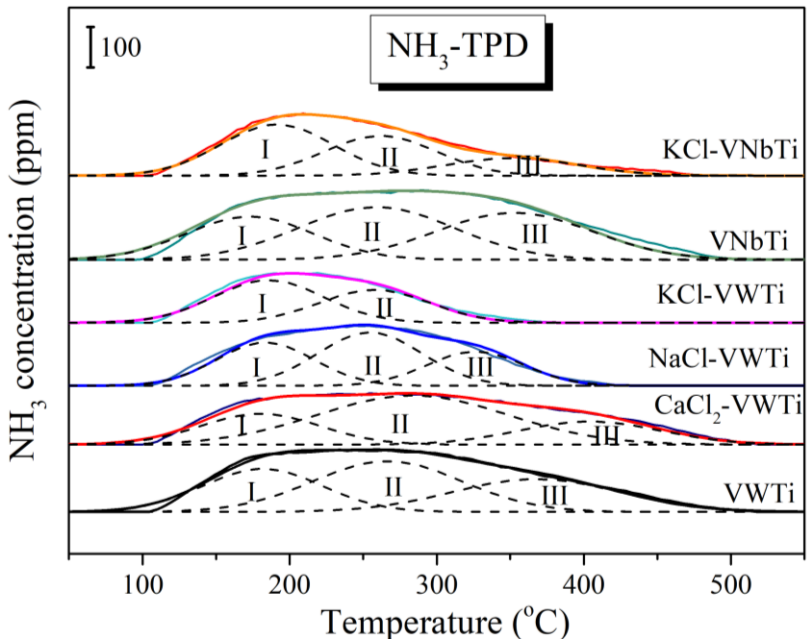

Fig. 3 NH_3-TPD profiles of the VWTi, VNbTi and corresponding poisoned catalysts

Table 3 Quantitative data of NH_3-TPD profiles over the studied catalysts

Sample	Peak temperature (°C)			Acid amount (μmol/g)			Acid amount (μmol/g)
	T_1	T_2	T_3	S_1	S_2	S_3	$S_1+S_2+S_3$
VWTi	179	269	369	70	102	74	246
$CaCl_2$-VWTi	179	284	403	50	127	44	221
NaCl-VWTi	184	254	329	57	76	45	178
KCl-VWTi	184	259	/	64	49	/	113
VNbTi	175	259	358	74	111	99	284
KCl-VNbTi	189	264	354	78	61	32	171

3.4 Redox performance (H_2-TPR)

The reducibility of the catalysts was tested by H_2-TPR experiments, and the results are shown as Fig. 4. The two peaks on VWTi catalyst at 471 ºC and 528 ºC can be assigned to the reduction of V^{5+} to V^{3+} [16, 42] and of W^{6+} to W^{4+} [43, 44], respectively. After poisoning with $CaCl_2$, the reduction peak of V^{5+} is partially affect in intensity while no evident effect on the reducibility of W^{6+} is seen. A new reduction peak at 700 ºC appears. This has been interpreted in terms of the bonding of WO_3 with Ca to form a stable W-O-Ca structure, which required a higher temperature to reduction than WO_3 [45]. This is not evident in our experiment, since the reduction peak of W^{6+} is unchanged after $CaCl_2$ poisoning.

As for NaCl-VWTi and KCl-VWTi catalysts, the H_2-TPR peak related to the reduction V^{5+} is apparently shifted to 500 ºC, and a small decrease in the reduction of W^{6+} is seen (peak at 528 ºC). A new peak at 595 ºC is formed (with an evident shoulder at 622 ºC for KCl-VWTi), which could be related to the interaction of the VO_x phase with NaCl and KCl. These results show that the three alkali (earth) chlorides affect the reducibility of V^{5+} and W^{6+} in a different extent, forming species with higher reduction temperature which depends on the nature of the cation (Na^+/K^+ vs Ca^{2+}). As we known, the active phase in VWTi catalyst is V_2O_5, while WO_3 acts as a promoter, with electronic and structural effect [46, 47]. The sample with higher activity ($CaCl_2$-VWTi) is the one characterized by a lower effect on V^{5+} reducibility and apparently unaffected redox properties of W^{6+}.

For VNbTi catalyst, the reduction peaks of V^{5+} and Nb^{5+} are observed at 460 ºC and 508 ºC [42, 48, 49]. Compared to VWTi catalyst, the reduction peak of V^{5+} is shifted to a lower temperature, suggesting that the replacement of WO_3 by Nb_2O_5 would enhance the reducibility of the catalyst as a consequence of an electronic effect. After KCl poisoning, new peaks are observed between 550 and 650 ºC, while the two peaks related to V^{5+} and Nb^{5+} reduction are very similar to VNbTi catalyst. As seen in $CaCl_2$-VWTi, the peak related to V^{5+} reduction seems more affected in

terms of intensity with respect to the promoter one, but is still present.

This would suggest a weak interaction of KCl with the catalyst surface, scarcely affecting the redox properties of active phase and promoter, indicating a more positive effect of Nb_2O_5, with respect to WO_3 to preserve the redox properties of V_2O_5 species in the presence of the pollutant. This is apparently in contrast with the Raman results, showing the disappearance of the V=O vibrations after KCl poisoning. Further studies, supported by theoretical calculations, would be necessary to explain this effect with a structural model.

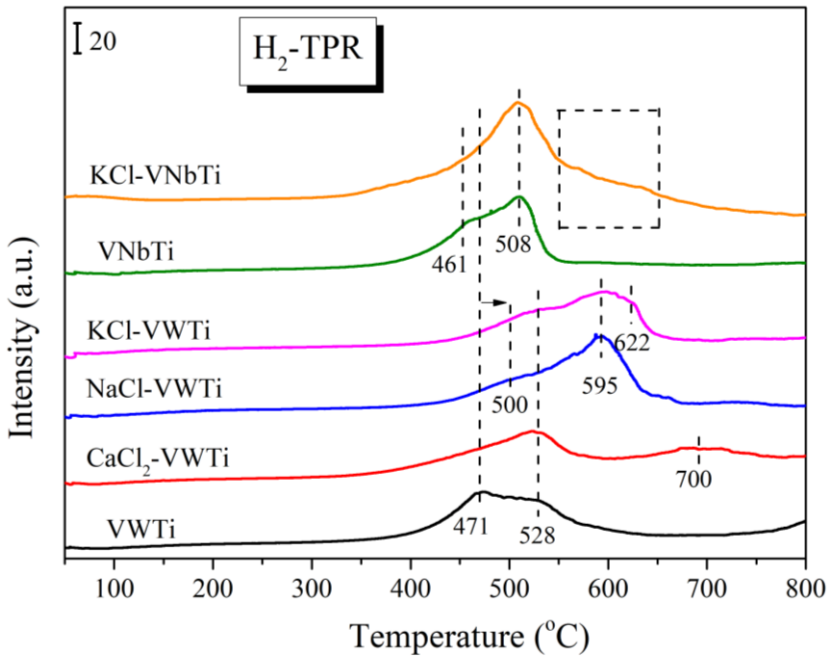

Fig. 4 H_2-TPR profiles of VWTi, VNbTi and corresponding alkali and earth alkali metal poisoned catalysts

3.5 The surface compositions (XPS)

Fig.S3(a) reports the Ti 2p spectra of VWTi, VNbTi, and corresponding poisoned catalysts. All catalysts displayed two bands at 464.4 eV and 458.7 eV, which were assigned to Ti $2p_{1/2}$ and Ti $2p_{3/2}$, respectively [50, 51]. This indicates that Ti mainly exists as Ti^{4+} on the surface of these catalysts, and $CaCl_2$, $NaCl_2$, and KCl had little effect on Ti^{4+} reducibility.

The W 4f XPS spectra of the VWTi, CaCl-VWTi, NaCl-VWTi, and KCl-VWTi catalysts are displayed in Fig.S3(b). All samples show two peaks at 37.3 eV and 35.2 eV, which can be assigned to surface W^{6+} species [52, 53], hardly affected by poisoning.

Fig.5(a) shows the $V2p_{3/2}$ spectra of these catalyst series. As can be seen, V $2p_{3/2}$ spectra of all samples could be divided into three peaks at 517.3 eV, 516.6 eV, and 515.7 eV, which were assigned to V^{5+}, V^{4+}, and V^{3+}, respectively [54, 55]. According to the literature, the $V^{5+}/(V^{5+}+V^{4+}+V^{3+})$ ratio can be used as a descriptor for the catalytic activity [53, 54, 56]. The $V^{5+}/(V^{5+}+V^{4+}+V^{3+})$ ratios calculated in the present work for all catalysts are listed in Table 3, together with the surface composition estimated by XPS. The measured surface atomic percentage is in good agreement with the expected composition of the samples. Coming to the V^{5+} ratio, this is 0.3 for VWTi catalyst, and decreases in the order $CaCl_2$-VWTi>NaCl-VWTi>KCl-VWTi, in agreement with the trends observed with the catalytic tests and H_2-TPR. This further supports the observation that the presence of KCl and NaCl has a stronger effect on redox properties of V_2O_5, resulting in a lower V^{5+} ratio, in agreement with DFT calculations [17, 18].

For VNbTi catalyst, the ratio of V^{5+} was 0.34 which was larger than that of VWTi catalyst, and decreased to 0.30 after KCl poisoning. These results are also in line with H_2-TPR results and could explain the higher activity of VNbTi in terms of an electronic effect of the promoter, which also induces a better resistance of KCl than VWTi catalyst.

O1s XPS spectra of VWTi catalyst displayed two bands, as shown as Fig.5 (b). In detail, the band at 529.9 eV labeled as O_β was related to lattice oxygen O^{2-}, which could be attributed to Ti-O, W-O, and V-O groups [45, 57]. The band at 531.3 eV labeled as O_α was related to the surface adsorbed oxygen [58, 59]. O_α species have been explained as hydroxyl groups and O_2^{2-}/O^- in the oxide defects, with alleged high mobility, which could promote the activation of adsorbed species (NO_x and NH_3 species), resulting in higher activity [60, 61]. Therefore, the ratio of O_α (*i.e.*, $(O_\alpha/(O_\alpha+ O_\beta))$ over these catalysts was calculated, and the results are listed in Table 3. It was found that

the O_α ratio of VWTi catalyst was as high as 0.42, and it decreased to 0.32, 0.31 and 0.27 after introducing $CaCl_2$, NaCl, and KCl, respectively. The O_α ratio of Nb_2O_5 catalysts was slightly higher than the corresponding WO_3 ones: 0.43 and 0.33 in VNbTi and KCl-VNbTi catalysts, respectively. The observed trend is in agreement with the activity of the catalyst, but cannot explain alone the observed loss of activity after poisoning.

Finally, it is interesting to notice that in $CaCl_2$-VWTi catalyst, O_α and O_β are shifted to a lower binding energy with respect to the others. This would suggest an increase in the electron cloud density around the O atom, which could facilitate the electron transfer, thus explaining the higher activity with respect to NaCl-VWTi and KCl-VWTi catalysts.

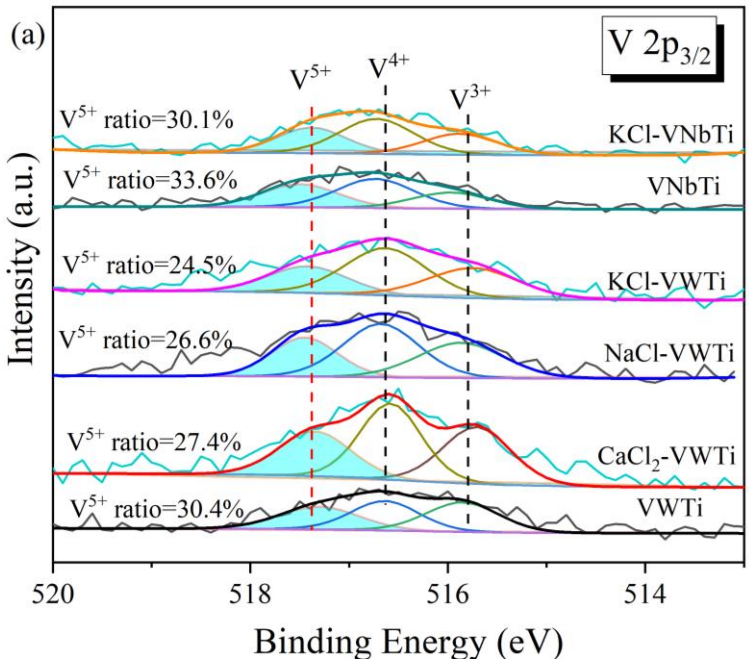

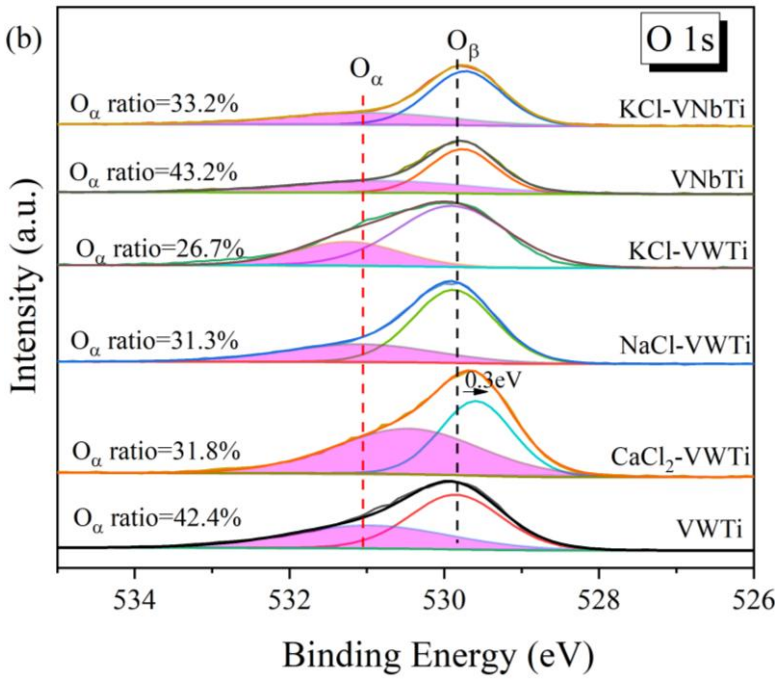

Fig. 5 (a) V $2p_{3/2}$ and (b) O 1s XPS spectra of the VWTi, VNbTi and corresponding poisoned catalysts.

Table 4 Surface composition (atomic percentage), $O_\alpha/(O_{tot})$ and $V^{5+}/(V_{tot})$ surface ratios of the catalysts.

Sample	V	W	Ti	O	K	Na	Ca	Cl	Nb	O_α	V^{5+}
	Atomic %									ratio	
VWTi	3.67	4.68	22.41	69.24	/	/	/	/	/	0.42	0.30
$CaCl_2$-VWTi	3.23	4.32	23.25	66.70	/	/	0.89	1.41	/	0.32	0.27
NaCl-VWTi	3.42	4.53	22.96	67.11	/	0.93	/	1.05	/	0.31	0.27
KCl-VWTi	3.35	4.46	21.96	68.27	1.02	/	/	0.94	/	0.27	0.25
VNbTi	3.83	/	20.40	70.1	/	/	/	/	5.67	0.43	0.34
KCl-VNbTi	3.72	/	21.63	67.23	1.06	/	/	0.98	5.38	0.33	0.30

3.6 Analysis of the surface adsorbed species by in-situ DRIFTS

In-situ DRIFT spectroscopy was used to explore the effect of the alkali and alkaline earth

metal chlorides and replacement of WO_3 by Nb_2O_5 on the surface species formed by interaction of the catalysts surface with the NH_3-SCR reactants. *In-situ* FTIR coupled to CO adsorption was used to assess the dispersion of the alkali and alkaline earth metal ions on the poisoned VWTi and VNbTi catalysts.

3.6.1 In-situ DRIFTS of NH_3 adsorption

NH_3 adsorption followed by *in-situ* infrared spectroscopy provides qualitative information about the nature of acid surface sites, responsible for the NH_3-TPD profiles described above. Fig. 5 shows the effect of $CaCl_2$, NaCl, and KCl and replacement of WO_3 by Nb_2O_5 on Brønsted (B) and Lewis (L) acid sites of VWTi catalyst. For VWTi catalyst, two bands appeared at 1678 cm^{-1} and 1440 cm^{-1} after NH_3 saturation at 50 ^oC, which were assigned to NH_4^+ species formed by interaction of NH_3 with (V-OH) Brønsted acid sites [15, 62, 63]. After poisoning, the intensity of this band is considerably lowered in the order $CaCl_2$>NaCl>KCl, in agreement with the observed changes in NH_3-TPD (Figure 3 and Table 3) and DFT calculations indicating that the cations are substituting a V-OH group [17, 18]. Moreover, a new band appeared at 1602 cm^{-1} in the characteristic region of NH_3 adsorbed on Lewis acid. A similar band has been however assigned to NH_3 interacting with Cl^- anions. [19, 64]. Kong et al [19] compared the effect of KCl and K_2O on V_2O_5-WO_3/TiO_2 catalysts, and reported about a competition for NH_3 between Cl^- and V_2O_5. The higher deactivation of KCl poisoned catalyst with respect to K_2O ones was thus explained by the scarce reactivity of NH_3 molecules interacting with Cl^- anions instead of V_2O_5 and WO_3 species.

When WO_3 is replaced with Nb_2O_5, the intensity of NH_4^+ species at 1440 and 1678 cm^{-1} increased and a new band appeared at 1235 cm^{-1} related to NH_3 species adsorbed on L acid sites [65]. The change in the NH_4^+ and NH_3 bands after poisoning with KCl is evident, but less important than that of KCl-VWTi catalyst. These observations are in agreement with the NH_3-TPD data, testifying of an improvement in surface acidity and lower effect of KCl when Nb_2O_5 replaced WO_3 as a promoter.

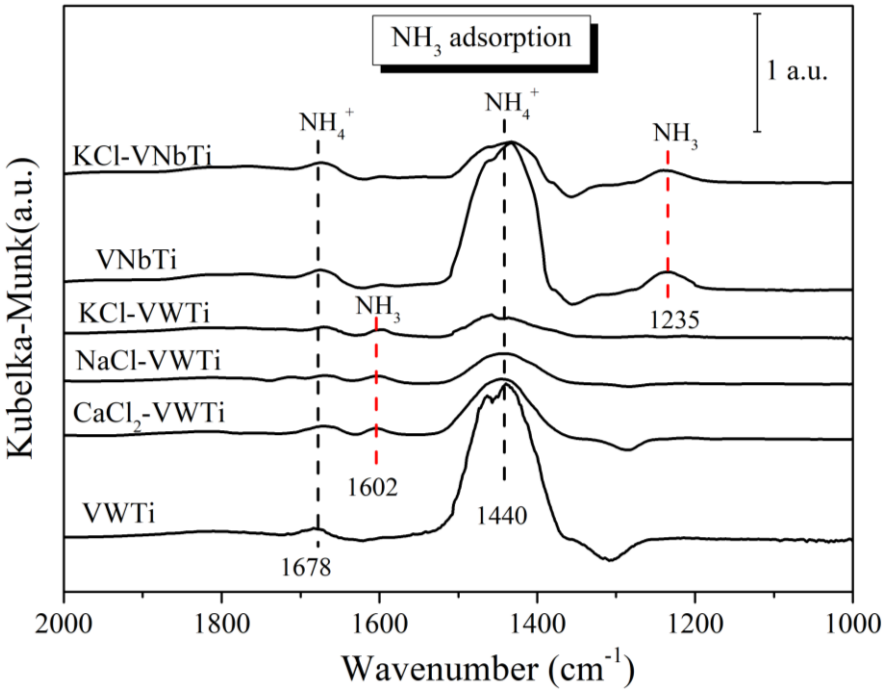

Fig. 5 *In-situ* DRIFTS of NH_3 adsorption at 50 °C on the VWTi and VNbTi and corresponding poisoned catalysts

3.6.2 In-situ DRIFTS of NO+O₂ adsorption

The effect of $CaCl_2$, NaCl, and KCl on the adsorption of NO_x species was characterized by *in-situ* DRIFTS of $NO+O_2$ adsorption, and the results are shown in Fig.6. For VWTi catalyst, broad band at 1627 cm^{-1} with a very weak peak around 1577 cm^{-1} is observed after $NO+O_2$ saturation at 50 °C. This was attributed to adsorbed NO_2 species (1627 cm^{-1}) [66, 67], with a small contribution of chelating bidentate nitrates (1608/1577 cm^{-1}) [68]. The components at 1608 and 1577 cm^{-1} assigned to chelating bidentate nitrates becomes more evident after poisoning, at the expenses of adsorbed NO_2, particularly in KCl-VWTi catalyst. Moreover, for NaCl-VWTi and KCl-VWTi catalysts, a new intense absorption at 1408 and 1387 cm^{-1} assigned to monodentate nitrites appeared [69]. These results suggest that the introduction of these alkali metal chlorides would increase the adsorption sites of NO_x, while changing the reactivity of NO/O_2 mixture with the surface. According to literature [70, 71], the nitrites and nitrates formed by alkali metals are stable, not playing a role in the NH_3-SCR reaction. Indeed, adsorbed monodentate nitrites are still present

at 225 °C on NaCl-VWTi and KCl-VWTi, while VWTi and $CaCl_2$-VWTi at the same temperature only show traces of adsorbed NO_2 (band at 1627 cm^{-1}, Fig. S4).

For VNbTi catalyst, only a well defined band assigned to adsorbed NO_2 species at 1627 cm^{-1} is present, which showed lower thermal stability with respect to VWTi (175 °C and 225 °C, Fig. S4). This would be in agreement with fact that VWTi also showed the formation of a small amount of more stable surface nitrates. After KCl poisoning, chelating bidentate nitrates (1608 and 1577 cm^{-1}) are formed together with adsorbed NO_2, in similar amount as in $CaCl_2$-VWTi catalyst. The thermal stability of these species is lower with respect to what observed on the poisoned VWTi catalysts (200 °C, Fig. S4). This is an interesting result, showing that Nb_2O_5 inhibited the formation of stable nitrates and particularly nitrites, which are formed in the presence of KCl on VWTi.

Finally, We notice that there is no apparent correlation between the surface reactivity of NO/O_2 and the relative amount of O_α measured by XPS.

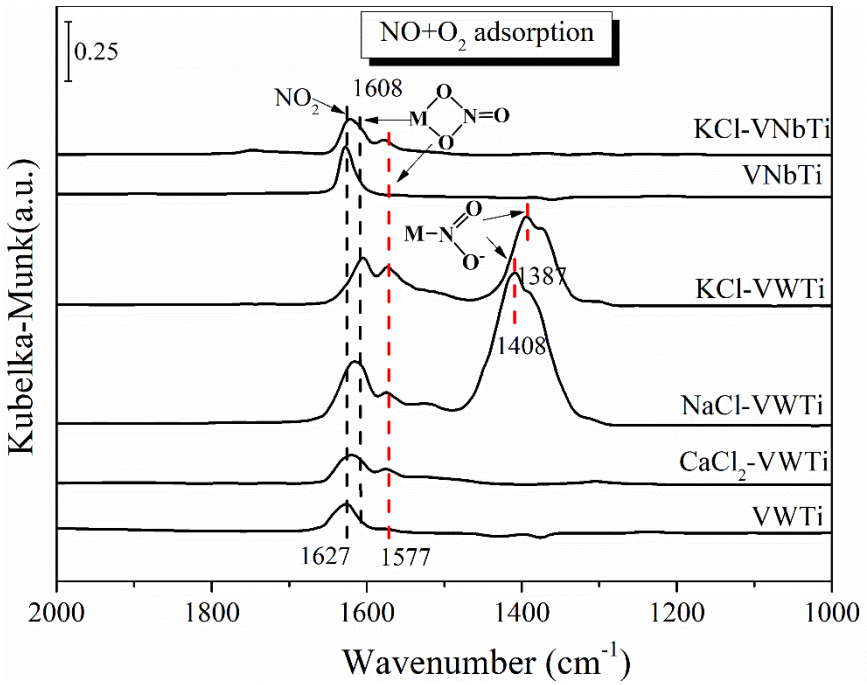

Fig. 6 *In-situ* DRIFTS of $NO+O_2$ adsorption at 50 °C on the VWTi and VNbTi catalysts and corresponding and poisoned catalysts

When NO/O_2 are co-adsorbed with NH_3 on the same set of catalysts, the resulting spectra are very similar to what reported in Fig. 5: apart from some differences in some peak position and

intensity, the spectra are mainly related to adsorbed NH_4^+ and NH_3 species (Fig. S5). This suggests an Eley-Rideal mechanism, where adsorbed NH_3 plays a key role [64].

3.6.3 In-situ FTIR study of CO adsorption

CO adsorption studies were carried out in static conditions, to probe the dispersion of the alkali and alkaline earth metal ions on the surface of VWTi and VNbTi catalysts. Spectra were measured at liquid nitrogen temperature, by stepwise decrease of the CO pressure in equilibrium with the pellet. Fig. 7a shows the corresponding spectra on VWTi catalyst, which are characterized by peaks at 2193 cm^{-1} (moving at 2198 cm^{-1} at low CO coverage), 2169 and 2142 cm^{-1}. The band at 2140/2142 cm^{-1} is related to the so-called 'liquid-like', which is aspecific being related to CO condensation on the surface or inner porosity of the materials. Its intensity varies in the different samples, but will not be discussed in detail due to its aspecificity.

The bands at 2169 and 2193/2198 cm^{-1} can be related to CO interacting with V-OH groups and with W^{x+} ions (X=5 or 6) [31]. After introducing $CaCl_2$, the intensity of CO bands becomes weaker, and no signal related to the formation of Ca^{2+}·· CO adducts is observed. In agreement with Raman and H_2-TPR results, this would indicate a weak interaction of the cation with the active phase and promoter. Importantly, V-OH groups are still present in the sample (V-OH·· CO band at 2169 cm^{-1} and Figure S6), in agreement with NH_3-TPD results, suggesting that the Ca^{2+} ions are not able to exchange the proton, at variance with what reported for monovalent cations [17, 18].

Interestingly, the CO band at 2169 cm^{-1} disappeared after introducing NaCl and KCl, which can be related to a strong interaction of the cations with then active phase, forming VO-Na/K structures, at the expenses of V-OH species (see also Fig. S6 for the OH stretching region). This interaction also affects the W^{x+} ions, which are no more able to interact with CO (band at 2193/2198 cm^{-1}). This could be related to the disappearance of the tungstenyl bands in the corresponding Raman spectra. In both cases new intense bands related to the interaction of CO with

Na^+ and K^+ appeared at 2165 and 2155 cm^{-1}, respectively [72, 73]. This suggests that the cations, probably present in VO-K/Na structures, are coordinatively unsaturated, i.e., have Lewis acid character.

The spectra measured on VNbTi catalysts show the same aspecific band at 2142 cm^{-1}, a stable band at 2185 cm^{-1} (not disappearance upon decreasing CO equilibrium pressure) and a relatively weaker one at 2165 cm^{-1}. The band at 2165 cm^{-1} can be related to V-OH·· CO adducts, in lower amount and slightly different acidity with respect to VWTi (Fig. S6), and the stable one at 2185 cm^{-1} to the interaction of CO with surface Nb^{x+} sites. After KCl poisoning these bands disappear, and a strong band due to K^+·· CO adducts is observed at 2156 cm^{-1}. This shows an higher intensity with respect to what observed on KCl-VWTi, indicating a higher dispersion and/or accessibility of the alkali metal ions.

As mentioned above, it is important to notice that the surface OH groups (giving upon CO interaction a broad band within 3400~3600 cm^{-1}, Fig. S6) [31] completely disappeared after KCl and NaCl poisoning in VWTi catalyst, in agreement with the hypothesis that they substitute Brønsted V-OH groups [17, 18]. This does not occur in $CaCl_2$-VWTi catalyst, and is less evident in KCl-VNbTi, indicating that the replacement of WO_3 with Nb_2O_5 can in part protect surface Brønsted V-OH groups from KCl exchange, which is in agreement with the results of *In-situ* DRIFTS of NH_3 adsorption and NH_3-TPD. As a final comment, these results clearly show a different interaction of the cations with the surface of the catalysts, which seems to be mainly dependent on the cation charge. However, they do not shed light on the positive effect of Nb_2O_5 (*vs* WO_3) on catalytic activity and resistance to pollutants.

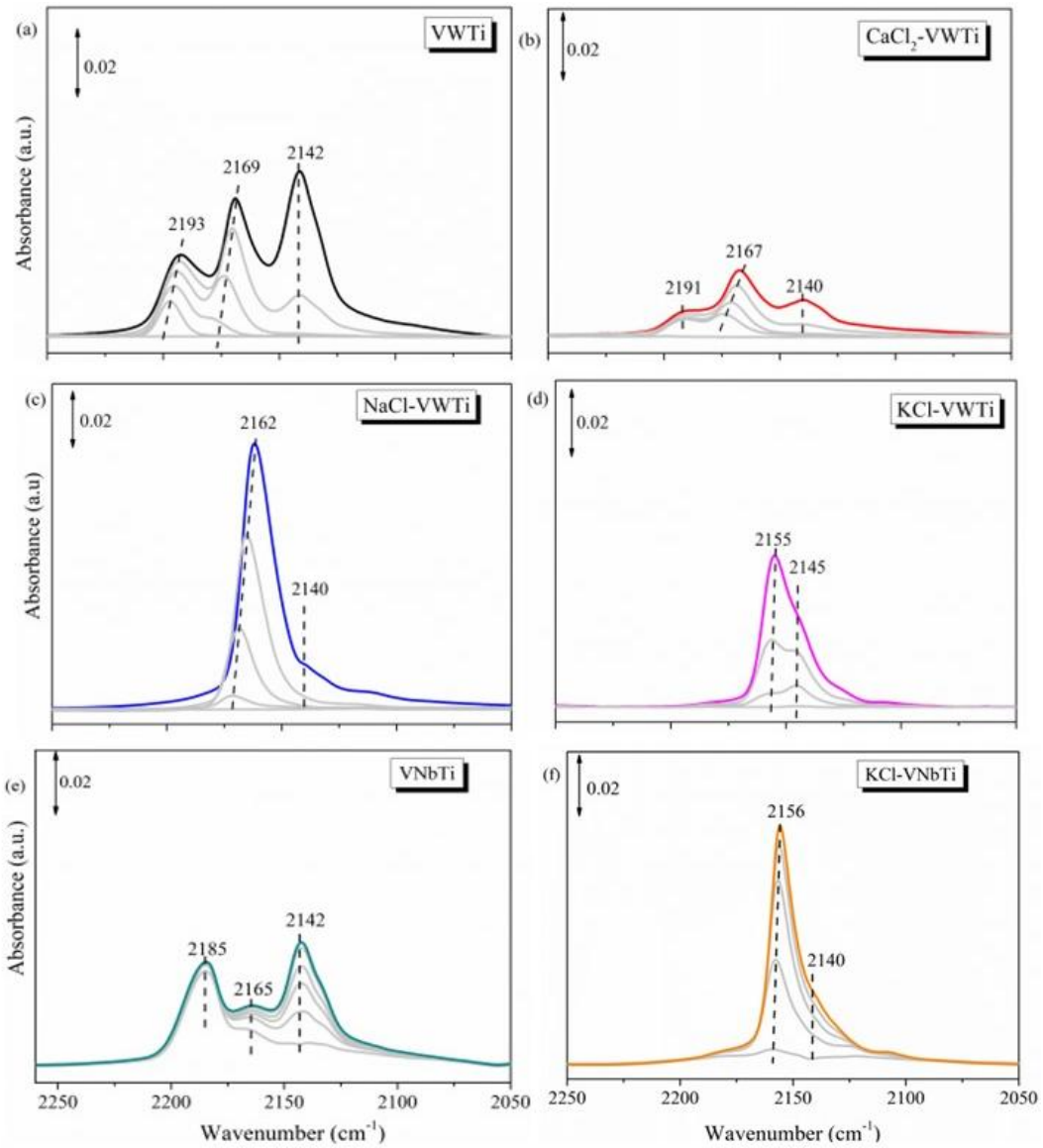

Fig. 7 *In-situ* FTIR spectra of CO adsorbed at liquid nitrogen temperature on the VWTi and VNbTi catalysts and corresponding poisoned catalysts. Maximum CO pressure 60 mbar.

4. Conclusion

In this work, we compared the effect of different alkali and earth alkali metal chlorides on V_2O_5-WO_3-TiO_2 catalyst to be used in the NH_3-SCR reaction for application in waste incineration plants. We find that KCl has the strongest poisoning effect, followed by NaCl, while the effect of $CaCl_2$ is milder. A detailed physico-chemical characterization points to the fact that the monovalent cations exchange Brønsted V-OH groups, while Ca^{2+} is less efficient in this reaction. All cations

affect the redox properties in a different extent (reducibility in hydrogen, surface V^{5+} and O_α relative amounts measured by XPS), but the better correlation with the catalytic activity seems to be found with the surface acidity, as measured by NH_3-TPD, and to the reactivity of NO/O_2 with the catalyst surface. In fact, the introduction of $CaCl_2$, NaCl, and KCl on V_2O_5-WO_3-TiO_2 favors the formation of stable nitrates and nitrites, which are probably not relevant in the NH_3-SCR reaction.

Using Nb_2O_5 as promoter instead of WO_3 increases the NOx conversion of the catalyst, its total surface acidity (NH_3-TPD) and its resistance to KCl pollution (chosen among the three due to highest deactivation observed on the V_2O_5-WO_3-TiO_2 catalyst). In the presence of this promoter KCl affects less strongly the redox properties of the catalysts, is less efficient in the exchange reaction with V-OH groups and does not promote the formation of stable nitrites. Even if we are not able to explain the phenomena at a molecular level, our results points to an electronic effect of the promoters in tuning the interaction of alkali and earth alkali metal chloride salts with the V_2O_5 active phase, thus influencing the catalyst performance.

Acknowledgments

The authors are grateful for support from the National Natural Science Foundation of China (No.52104322, 52174382). Jun Cao acknowledges the financial support from China scholarship Council.

References

[1] L.J. Ji, S.Y. Lu, J. Yang, C.C. Du, Z.L. Chen, A. Buekens, J.H. Yan, Municipal solid waste incineration in China and the issue of acidification: A review, Waste Manage. Res., 34 (2016) 280-297.

[2] J. Cao, X. Yao, F. Yang, L. Chen, M. Fu, C. Tang, L. Dong, Improving the denitration performance and K-poisoning resistance of the V_2O_5-WO_3/TiO_2 catalyst by Ce^{4+} and Zr^{4+} co-doping,

Chin. J. Catal., 40 (2019) 95-104.

[3] X.Q. Wang, Y. Liu, Z.B. Wu, The poisoning mechanisms of different zinc species on a ceria-based NH_3-SCR catalyst and the co-effects of zinc and gas-phase sulfur/chlorine species, J. Colloid. Interf. Sci., 566 (2020) 153-162.

[4] S.C. Xiong, J.J. Chen, N. Huang, T. Yan, Y. Peng, J.H. Li, The poisoning mechanism of gaseous HCl on low-temperature SCR catalysts: MnO_x-CeO_2 as an example, Appl. Catal. B., 267 (2020) 118668.

[5] L. Chen, X.J. Yao, J. Cao, F.M. Yang, C.J. Tang, L. Dong, Effect of Ti^{4+} and Sn^{4+} co-incorporation on the catalytic performance of CeO_2 -MnO_x catalyst for low temperature NH_3-SCR, Appl. Surf. Sci., 476 (2019) 283-292.

[6] E. Park, M. Kim, H. Jung, S. Chin, J. Jurng, Effect of sulfur on Mn/Ti catalysts prepared ssing chemical vapor condensation (CVC) for low-temperature NO reduction, ACS Catal., 3 (2013) 1518-1525.

[7] Z. Fei, Y. Yang, M. Wang, Z. Tao, Q. Liu, X. Chen, M. Cui, Z. Zhang, J. Tang, X. Qiao, Precisely fabricating Ce-O-Ti structure to enhance performance of Ce-Ti based catalysts for selective catalytic reduction of NO with NH_3, Chem. Eng. J., 353 (2018) 930-939.

[8] S.J. Yang, S.C. Xiong, Y. Liao, X. Xiao, F.H. Qi, Y. Peng, Y.W. Fu, W.P. Shan, J.H. Li, Mechanism of N_2O formation during the low-temperature selective catalytic reduction of NO with NH_3 over Mn-Fe spinel, Environ. Sci. Technol., 48 (2014) 10354-10362.

[9] S. Deng, T. Meng, B. Xu, F. Gao, Y. Fan, Advanced MnO_x/TiO_2 catalyst with preferentially exposed anatase {001} facet for low-temperature SCR of NO, ACS Catal., 6 (2016) 5807-5815.

[10] Y. Zheng, A.D. Jensen, J.E. Johnsson, J.R. Thøgersen, Deactivation of V_2O_5-WO_3-TiO_2 SCR catalyst at biomass fired power plants: Elucidation of mechanisms by lab and pilot-scale experiments, Appl. Catal. B., 83 (2008) 186-194.

[11] L. Pang, C. Fan, L.N. Shao, J.X. Yi, X. Cai, J. Wang, M. Kang, T. Li, Effect of V_2O_5/WO_3-TiO_2

catalyst preparation method on NO_x removal from diesel exhaust, Chin. J. Catal., 35 (2014) 2020-2028.

[12] X.X. Wang, Q.L. Cong, L. Chen, Y. Shi, Y. Shi, S.J. Li, W. Li, The alkali resistance of CuNbTi catalyst for selective reduction of NO by NH_3: A comparative investigation with VWTi catalyst, Appl. Catal. B., 246 (2019) 166-179.

[13] X. Wang, H. Ma, Y. Shi, Q. Wang, P. Xu, W. Li, S. Li, Regeneration of alkali poisoned TiO2-based catalyst by various acids in NO selective catalytic reduction with NH_3, Fuel, 285 (2021) 119069.

[14] C.U.I. Odenbrand, $CaSO_4$ deactivated V_2O_5-WO_3/TiO_2 SCR catalyst for a diesel power plant. Characterization and simulation of the kinetics of the SCR reactions, Appl. Catal. B., 234 (2018) 365-377.

[15] D. Nicosia, I. Czekaj, O. Krocher, Chemical deactivation of V_2O_5/WO_3-TiO_2 SCR catalysts by additives and impurities from fuels lubrication oils and urea solution-Part II. Characterization study of the effect of alkali and alkaline earth metals, Appl. Catal. B., 77 (2008) 228-236.

[16] L. Chen, J. Li, M. Ge, The poisoning effect of alkali metals doping over nano V_2O_5-WO_3/TiO_2 catalysts on selective catalytic reduction of NO_x by NH_3, Chem. Eng. J., 170 (2011) 531-537.

[17] X. Du, X. Gao, K. Qiu, Z. Luo, K. Cen, The Reaction of poisonous alkali oxides with vanadia SCR catalyst and the afterward influence: A DFT and experimental study, J. Phys. Chem. C, 119 (2015) 1905-1912.

[18] Y. Peng, J. Li, W. Shi, J. Xu, J. Hao, Design strategies for development of SCR catalyst: Improvement of alkali poisoning resistance and novel regeneration method, Environ. Sci. Technol., 46 (2012) 12623-12629.

[19] M. Kong, Q. Liu, J. Zhou, L. Jiang, Y. Tian, J. Yang, S. Ren, J. Li, Effect of different potassium species on the deactivation of V_2O_5-WO_3/TiO_2 SCR catalyst: Comparison of K_2SO_4, KCl and K_2O, Chem. Eng. J., 348 (2018) 637-643.

[20] Z.H. Lian, F.D. Liu, H. He, X.Y. Shi, J.S. Mo, Z.B. Wu, Manganese-niobium mixed oxide catalyst for the selective catalytic reduction of NO_x with NH_3 at low temperatures, Chem. Eng. J., 250 (2014) 390-398.

[21] S.P. Ding, F.D. Liu, X.Y. Shi, H. He, Promotional effect of Nb additive on the activity and hydrothermal stability for the selective catalytic reduction of NO_x with NH_3 over $CeZrO_x$ catalyst, Appl. Catal. B., 180 (2016) 766-774.

[22] Z.R. Ma, X.D. Wu, Z.C. Si, D. Weng, J. Ma, T.F. Xu, Impacts of niobia loading on active sites and surface acidity in NbO_x/CeO_2-ZrO_2 NH_3-SCR catalysts, Appl. Catal. B., 179 (2015) 380-394..

[23] R.Y. Qu, Y. Peng, X.X. Sun, J.H. Li, X. Gao, K.F. Cen, Identification of the reaction pathway and reactive species for the selective catalytic reduction of NO with NH_3 over cerium-niobium oxide catalysts, Catal. Sci. Technol., 6 (2016) 2136-2142.

[24] M. Casapu, O. Krocher, M. Mehring, M. Nachtegaal, C. Borca, M. Harfouche, D. Grolimund, Characterization of Nb-containing MnO_x-CeO_2 catalyst for low-temperature selective catalytic reduction of NO with NH_3, J. Phys. Chem. C, 114 (2010) 9791-9801.

[25] Z.R. Ma, D. Weng, X.D. Wu, Z.C. Si, B. Wang, A novel Nb-Ce/WO_x-TiO_2 catalyst with high NH_3-SCR activity and stability, Catal. Commun., 27 (2012) 97-100.

[26] M. Casapu, A. Bernhard, D. Peitz, M. Mehring, M. Elsener, O. Krocher, A Niobia-Ceria based multi-purpose catalyst for selective catalytic reduction of NO_x, urea hydrolysis and soot oxidation in diesel exhaust, Appl. Catal. B., 103 (2011) 79-84.

[27] R.Y. Qu, X. Gao, K.F. Cen, J.H. Li, Relationship between structure and performance of a novel cerium-niobium binary oxide catalyst for selective catalytic reduction of NO with NH_3, Appl. Catal. B., 142 (2013) 290-297.

[28] J. Cao, X.J. Yao, L. Chen, K.K. Kang, M. Fu, Y. Chen, Effects of different introduction methods of Ce^{4+} and Zr^{4+} on denitration performance and anti-K poisoning performance of V_2O_5-WO_3/TiO_2 catalyst, J. Rare Earths, 38 (2020) 1207-1214.

[29] X. Yao, R. Zhao, L. Chen, J. Du, C. Tao, F. Yang, L. Dong, Selective catalytic reduction of NO_x by NH_3 over CeO_2 supported on TiO_2: Comparison of anatase, brookite, and rutile, Appl. Catal. B., 208 (2017) 82-93.

[30] J. Cao, W.Z. Liu, K.K. Kang, L. Chen, X. Qiao, X.J. Yao, Effects of the morphology and crystal-plane of TiO_2 on NH_3-SCR performance and K tolerance of V_2O_5-WO_3/TiO_2 catalyst, Appl. Catal. A., 623 (2021) 118285.

[31] Y. Ganjkhanlou, T.V.W. Janssens, P.N.R. Vennestrom, L. Mino, M.C. Paganini, M. Signorile, S. Bordiga, G. Berlier, Location and activity of VO_x species on TiO_2 particles for NH_3-SCR catalysis, Appl. Catal. B., 278 (2020) 119337.

[32] I. Boldog, P. Cicmanec, Y. Ganjkhanlou, R. Bulanek, Surfactant templated synthesis of porous VO_x-ZrO_2 catalysts for ethanol conversion to acetaldehyde, Catal. Today, 304 (2018) 64-71.

[33] L. Nakka, J.E. Molinari, I.E. Wachs, Surface and bulk aspects of mixed oxide catalytic nanoparticles: oxidation and dehydration of CH_3OH by polyoxometallates, J. Am. Chem. Soc., 131 (2009) 15544-15554.

[34] S.S.R. Putluru, L. Schill, A. Godiksen, R. Poreddy, S. Mossin, A.D. Jensen, R. Fehrmann, Promoted V_2O_5/TiO_2 catalysts for selective catalytic reduction of NO with NH_3 at low temperatures, Appl. Catal. B, 183 (2016) 282-290.

[35] M.A. Banares, I.E. Wachs, Molecular structures of supported metal oxide catalysts under different environments, J. Raman Spectrosc., 33 (2002) 359-380.

[36] M.A. Vuurman, I.E. Wachs, A.M. Hirt, Structural determination of supported V_2O_5-WO_3/TiO_2 catalysts by in-situ Raman spectroscopy and X-ray photoelectron spectrosocopy, J. Phys. Chem., 95 (1991) 9928-9937.

[37] J.K. Lai, I.E. Wachs, A perspective on the selective catalytic reduction (SCR) of NO with NH_3 by Supported V_2O_5-WO_3/TiO_2 Catalysts, ACS Catal., 8 (2018) 6537-6551.

[38] N.Y. Topsoe, Mechanism of the selective catalytic reduction of nitric-oxide by ammonia by in-

situ online fourier-transform inftared-soectroscopy, Science, 265 (1994) 1217-1219.

[39] J. Cao, Z.Q. Lu, L.M. Teng, X. Qiao, W.Z. Liu, H.L. Wu, L.J. Jiang, Q.R. Wu, Q.C. Liu, The combination effects of K_2O and PbO poisoning on NH_3-SCR TiO_2-CeO_2 catalyst, J. Environ. Chem. Eng., 9 (2021) 106127.

[40] K.A. Michalow-Mauke, Y. Lu, K. Kowalski, T. Graule, M. Nachtegaal, O. Krocher, D. Ferri, Flame-made WO_3/CeO_x-TiO_2 catalysts for selective catalytic reduction of NO_x by NH_3 , ACS Catal., 5 (2015) 5657-5672.

[41] Q. Wan, L. Duan, J. Li, L. Chen, K. He, J. Hao, Deactivation performance and mechanism of alkali (earth) metals on V_2O_5–WO_3/TiO_2 catalyst for oxidation of gaseous elemental mercury in simulated coal-fired flue gas, Catal. Today, 175 (2011) 189-195.

[42] Y. Peng, J. Li, W. Si, J. Luo, Y. Wang, J. Fu, X. Li, J. Crittenden, J. Hao, Deactivation and regeneration of a commercial SCR catalyst: Comparison with alkali metals and arsenic, Appl. Catal. B., 168-169 (2015) 195-202.

[43] P. Kompio, A. Bruckner, F. Hipler, G. Auer, E. Loffler, W. Grunert, A new view on the relations between tungsten and vanadium in V_2O_5-WO_3/TiO_2 catalysts for the selective reduction of NO with NH_3, J. Catal., 286 (2012) 237-247.

[44] X. Li, X. Li, J. Chen, J. Li, J. Hao, An efficient novel regeneration method for Ca-poisoning V_2O_5-WO_3/TiO_2 catalyst, Catal. Commun., 87 (2016) 45-48.

[45] X. Li, X.S. Li, J.H. Li, J.M. Hao, High calcium resistance of CeO_2-WO_3 SCR catalysts: Structure investigation and deactivation analysis, Chem. Eng. J., 317 (2017) 70-79.

[46] N.R. Jaegers, J.K. Lai, Y. He, E. Walter, D.A. Dixon, M. Vasiliu, Y. Chen, C.M. Wang, M.Y. Hu, K.T. Mueller, I.E. Wachs, Y. Wang, J.Z. Hu, Mechanism by which tungsten oxide promotes the activity of uupported V_2O_5/TiO_2 catalysts for NO_x abatement: Structural effects revealed by V-51 MAS NMR spectroscopy, Angew. Chem. Inter. Ed., 58 (2019) 12609-12616.

[47] K. Routray, W. Zhou, C.J. Kiely, I.E. Wachs, Catalysis science of methanol oxidation over iron

vanadate vatalysts: Nature of the catalytic active sites, ACS Catal., 1 (2011) 54-66.

[48] S.S. Liu, H. Wang, R.D. Zhang, Y. Wei, Synergistic effect of niobium and ceria on anatase for low-temperature NH_3-SCR of NO process, Mol. Catal., 478 (2019).

[49] W. Tan, C.Y. Wang, S.H. Yu, Y.B. Li, S.H. Xie, F. Gao, L. Dong, F.D. Liu, Revealing the effect of paired redox-acid sites on metal oxide catalysts for efficient NO_x removal by NH_3-SCR, J. Hazard. Mater., 416 (2021) 125826.

[50] J. Cao, Sohrab. Rohani, W.Z Liu, H.H Liu, Z.Q Lu, H.L Wu, L.J Jiang, M. Kong, Q.C. L, X.J Yao, Influence of phosphorus on the NH_3-SCR performance of CeO_2-TiO_2 catalyst for NO_x removal from co-incineration flue gas of domestic waste and municipal sludge, J. Colloid Interf. Sci. 610 (2022) 463-473.

[51] B. Shen, F. Wang, B. Zhao, Y. Li, Y. Wang, The behaviors of V_2O_5-WO_3/TiO_2 loaded on ceramic surfaces for NH_3-SCR, J. Ind. Eng. Chem., 33 (2016) 262-269.

[52] D. Ye, R. Qu, C. Zheng, K. Cen, X. Gao, Mechanistic investigation of enhanced reactivity of NH_4HSO_4 and NO on Nb- and Sb-doped VW/Ti SCR catalysts, Appl. Catal. A., 549 (2018) 310-319.

[53] J. Yang, Q. Yang, J. Sun, Q. Liu, D. Zhao, W. Gao, L. Liu, Effects of mercury oxidation on V_2O_5-WO_3/TiO_2 catalyst properties in NH_3-SCR process, Catal. Commun., 59 (2015) 78-82.

[54] N.Y. Topsoe, H. Topsoe, J.A. Dumesic, Vanadia/Titania Catalysts for Selective Catalytic Reduction (SCR) of Nitric-Oxide by Ammonia: I. Combined Temperature-Programmed in-Situ FTIR and On-line Mass-Spectroscopy Studies, J. Catal., 151 (1995) 226-240.

[55] X. Guo, C. Bartholomew, W. Hecker, L.L. Baxter, Effects of sulfate species on V_2O_5/TiO_2 SCR catalysts in coal and biomass-fired systems, Appl. Catal. B., 92 (2009) 30-40.

[56] H.P. Xiao, Y. Chen, C. Qi, Y. Ru, Effect of Na poisoning catalyst (V_2O_5-WO_3/TiO_2) on denitration process and SO_3 formation, Appl. Surf. Sci., 433 (2018) 341-348.

[57] Z. Liu, S. Zhang, J. Li, J. Zhu, L. Ma, Novel V_2O_5-CeO_2/TiO_2 catalyst with low vanadium

loading for the selective catalytic reduction of NO_x by NH_3, Appl. Catal. B., 158-159 (2014) 11-19.

[58] W.S. Hu, Y.H. Zhang, S.J. Liu, C.H. Zheng, X. Gao, I. Nova, E. Tronconi, Improvement in activity and alkali resistance of a novel V-$Ce(SO_4)_2$/Ti catalyst for selective catalytic reduction of NO with NH_3, Appl. Catal. B., 206 (2017) 449-460.

[59] X. Li, J.H. Li, Y. Peng, T. Zhang, S. Liu, J.M. Hao, Selective catalytic reduction of NO with NH_3 over novel iron-tungsten mixed oxide catalyst in a broad temperature range, Catal. Sci. Technol., 5 (2015) 4556-4564.

[60] Z. Liu, X. Feng, Z. Zhou, Y. Feng, J. Li, Ce-Sn binary oxide catalyst for the selective catalytic reduction of NO_x by NH_3, Appl. Surf. Sci., 428 (2018) 526-533.

[61] H.L. Li, C.Y. Wu, Y. Li, J.Y. Zhang, CeO_2-TiO_2 catalysts for catalytic oxidation of elemental mercury in low-rank coal combustion flue gas, Environ. Sci. Technol., 45 (2011) 7394-7400.

[62] P. Sun, R.T. Guo, S.M. Liu, S.X. Wang, W.G. Pan, M.Y. Li, S.W. Liu, J. Liu, X. Sun, Enhancement of the low-temperature activity of Ce/TiO_2 catalyst by Sm modification for selective catalytic reduction of NO_x with NH_3, Mol. Catal., 433 (2017) 224-234.

[63] A. Shi, X. Wang, T. Yu, M. Shen, The effect of zirconia additive on the activity and structure stability of V_2O_5/WO_3-TiO_2 ammonia SCR catalysts, Appl. Catal. B., 106 (2011) 359-369.

[64] J. Yang, S. Ren, R.J.G. Nuguid, D. Ferri, Q. Liu, O. Kröcher, Poisoning of Mn-Ce/AC catalysts for low-temperature NH_3-SCR of NO by K^+ and its counter-ions (Cl^-/NO_3^-/SO_4^{2-}), Appl. Catal. A., 638 (2022) 118636.

[65] N. Yang, R. Guo, W. Pan, Q. Chen, Q. Wang, C. Lu, The promotion effect of Sb on the Na resistance of Mn/TiO_2 catalyst for selective catalytic reduction of NO with NH_3, Fuel, 169 (2016) 87-92.

[66] Y. Liu, T.T. Gu, X.L. Weng, Y. Wang, Z.B. Wu, H.Q. Wang, DRIFT studies on the selectivity promotion mechanism of Ca-Modified Ce-Mn/TiO_2 catalysts for low-temperature NO reduction with NH_3, J. Phys. Chem. C, 116 (2012) 16582-16592.

[67] P. Sun, R. Guo, S. Liu, S. Wang, W. Pan, M. Li, S. Liu, J. Liu, X. Sun, Enhancement of the low-temperature activity of Ce/TiO_2 catalyst by Sm modification for selective catalytic reduction of NO_x with NH_3, Mol. Catal., 433 (2017) 224-234.

[68] C. Negri, P.S. Hammershoi, T.V.W. Janssens, P. Beato, G. Berlier, S. Bordiga, Investigating the Low Temperature Formation of Cu-II-(N,O) Species on Cu-CHA Zeolites for the Selective Catalytic Reduction of NO_x, Chem. Eur. J., 24 (2018) 12044-12053.

[69] Z.B. Wu, B.Q. Jiang, Y. Liu, H.Q. Wang, R.B. Jin, DRIFT study of manganese/titania-based catalysts for low-temperature selective catalytic reduction of NO with NH_3, Environ. Sci. Technol. 41 (2007) 5812-5817.

[70] K. Kang, X. Yao, J. Cao, Z. Li, J. Rong, W. Luo, W. Zhao, Y. Chen, Enhancing the K resistance of $CeTiO_x$ catalyst in NH_3-SCR reaction by CuO modification, J. Hazard. Mater., 402 (2021) 123551.

[71] X.J. Yao, K.K. Kang, J. Cao, L. Chen, W. Luo, W.X. Zhao, J. Rong, Y. Chen, Enhancing the denitration performance and anti-K poisoning ability of CeO_2-TiO_2/P25 catalyst by H_2SO_4 pretreatment: Structure-activity relationship and mechanism study, Appl. Catal. B, 269 (2020) 118808.

[72] A. Zecchina, D. Scarano, S. Bordiga, G. Ricchiardi, G. Spoto, F. Geobaldo, IR studies of CO and NO adsorbed on well characterized oxide single microcrystals, Catal. Today, 27 (1996) 403-435.

[73] D. Scarano, A. Zecchina, CO adsorption at -77 K on KCl films-an infraden incestigation, J. Chem. Soc., Faraday Trans. I, 82 (1986) 3611-3624.